Title

On the Differential Roles of Mg2+, Zn2+, and Cu2+ in the Equilibrium of β-N-Methyl-Amino-L-Alanine (BMAA) and its Carbamates

Journal

Neurotoxicity Research, 39(1)

ISSN

1029-8428

Authors

Diaz-parga, Pedro
Goto, Joy J
Krishnan, VV

Publication Date

2021-02-01

DOI

10.1007/s12640-019-00157-0

Peer reviewed

HHS Public Access

Author manuscript

Neurotox Res. Author manuscript; available in PMC 2022 February 01.

Published in final edited form as:

Neurotox Res. 2021 February ; 39(1): 6–16. doi:10.1007/s12640-019-00157-0.

On the differential roles of Mg^{2+}, Zn^{2+}, and Cu^{2+} in the equilibrium of β-N-methyl-amino-L-alanine (BMAA) and its Carbamates

Pedro Diaz-parga[#], **Joy J. Goto**[1,*], **V.V. Krishnan**[1,2,*]

[1]Department of Chemistry, California State University, Fresno CA 93740

[2]Department of Pathology & Laboratory Medicine, University of California Davis, Davis CA 95616

Abstract

β-N-methyl-amino-L-alanine (BMAA) in the presence of bicarbonate (HCO_3^-) undergoes structural modifications generating two carbamate species, α-carbamate and β-carbamate forms of BMAA. The chemical structure of BMAA and BMAA-carbamate adducts strongly suggest they may interact with divalent metal ions. The ability of BMAA to cross the blood-brain barrier and possibly interact with divalent metal ions may augment the neurotoxicity of these molecules. To understand the effects of divalent metal ions (Mg^{2+}, Zn^{2+}, and Cu^{2+}) on the overall dynamic equilibrium between BMAA and its carbamate adducts, a systematic study using nuclear magnetic resonance (NMR) is presented. The chemical equilibria between BMAA, its carbamate adducts, and each of the divalent ions were studied using two-dimensional chemical exchange spectroscopy (EXSY). The NMR results demonstrate that BMAA preferentially interacts with Zn^{2+} and Cu^{2+}, causing an overall reduction in the production of carbamate species by altering the dynamic equilibria. The NMR based spectral changes due to the BMAA interaction with Cu^{2+} is more drastic than with the Zn^{2+}, under the same stoichiometric ratios of BMAA and the individual divalent ions. However, the presence of Mg^{2+} does not significantly alter the dynamic equilibria between BMAA and its carbamate adducts. The NMR based results are further validated using circular dichroism (CD) spectroscopy observing the n→π interaction in the complex formation of BMAA and the divalent metal ions with additional verification of the interaction with Cu^{2+}, using UV-vis spectroscopy. Our results demonstrate that BMAA differentially interacts with divalent metal ions ($Mg^{2+} < Zn^{2+} < Cu^{2+}$), and thus alters the rate of formation of carbamate products. The equilibria between BMAA, the bicarbonate ions, and the divalent metal ions may alter the total population of a specific form of BMAA-ion complex at physiological conditions and, therefore, adds a level of complexity of the mechanisms by which BMAA acts as a neurotoxin.

Keywords

BMAA; carbamate formation; divalent metal ions; Nuclear Magnetic Resonance (NMR); Exchange Spectroscopy (EXSY)

[*]Correspondence to jgoto@csufresno.edu or krish@csufresno.edu.

[#]Currently Quantitative Biology Graduate Program, University of California, Merced.

Introduction

The nonproteinogenic amino acid β-N-methylamino-L-alanine (BMAA) is implicated in the onset of Amyotrophic Lateral Sclerosis/Parkinsonism-Dementia Complex (ALS/PDC). BMAA was derived initially from the cycad of Guam and is thought to be the primary cause of sporadic ALS among the Chamorro people of Guam (Bradley and Cox 2009; Bradley and Mash 2009; Murch et al. 2004a; Murch et al. 2004b; Vega 1967). Most genera of cyanobacteria can produce BMAA, resulting in a several-fold increase of BMAA in each trophic level (Chiu et al. 2013; Chiu et al. 2011; Cox et al. 2005). Because of BMAA's presence in the ecosystem, the exposure to and accumulation of BMAA over time may contribute to the progressive onset of ALS/PDC (Brand et al. 2010; Cox et al. 2005; Jonasson et al. 2010). Quantification of BMAA in the brain tissues of both Alzheimer's and ALS patients suggests that BMAA is an etiologic agent that contributes to neurodegeneration in the late stages of life (Chiu et al. 2011; Murch et al. 2004a; Murch et al. 2004b; Pablo et al. 2009). The ability of BMAA to sequester metal ions, coupled with the increasing role of divalent metal ions, Cu^{2+}, Zn^{2+}, Mg^{2+}, and Fe^{2+} in the pathogenesis of neurodegenerative disorders, suggests BMAA may cause metal dyshomeostasis in neuronal regions, resulting in neurological damage over the years.

In the presence of HCO_3^- or CO_2, BMAA undergoes structural modifications to form the carbamic acid functional group (NH_2COOH), at either the α-NH_2 or β-NH_2, producing two new neuroactive species (Weiss and Choi 1988). Formation of the carbamic acid (NH_2COOH), known as carbamylation, converts the biologically inert BMAA, to a biologically active carbamate adduct. Physiologically, the bicarbonate buffer system is utilized to remove and convert excess carbon dioxide (CO_2) produced from cellular respiration to carbonic acid (H_2CO_3) and bicarbonate (HCO_3). Modulation of the bicarbonate buffering system is necessary for regulating weak acid and base equilibria, to maintain the physiological pH at ~7.4.

The HCO_3^- and CO_2 produced by the bicarbonate buffer system can react with both deprotonated amines to produce carbamylated products (Figure 1). The complexation between the α-amine and β-amine with HCO_3^- was first investigated by Nunn and co-workers (Davis et al. 1993; Nunn and O'Brien 1989). Because of the similarity of the β-carbamate to glutamate, they hypothesized that the β-carbamate of BMAA is primarily responsible for the observed neurotoxicity. Characterization of the carbamate compounds was later investigated using nuclear magnetic resonance (NMR) spectroscopy, but the β-carbamate could not be detected by NMR due to a lack of spectral resolution of the spectrometer (Nunn and O'Brien 1989). A 1990 study by Myers and Nelson (Myers and Nelson 1990) utilized isotopically labeled sodium bicarbonate [^{13}C] $NaHCO_3$ to verify the presence of both the αcarbamate and the β-carbamate. Recently, we undertook a systematic evaluation of BMAA and HCO_3^- interaction using NMR spectroscopy with a particular focus on the chemical equilibrium process of the carbamate formation (Zimmerman et al. 2016). In addition to confirming the earlier observations that BMAA: HCO_3^- interactions led to the formation of both α– and β– carbamates, we observed that these adducts co-exist in the solution state, under physiological conditions.

Structurally, BMAA resembles other amino acids (e.g., glutamate), which implies it can be actively transported across the blood-brain barrier via amino acid transporters. Because BMAA can cross the blood-brain barrier (BBB), this can lead to the accumulation of free BMAA and result in neurological damage (Chiu et al. 2012; Choi 1988; Lobner et al. 2007; Richter and Mena 1989; Smith et al. 1992; Xie et al. 2013). The gradual accumulation of BMAA within the brain creates a reservoir of available BMAA that can interact within the motor cortex, prefrontal cortex, and hippocampus (Buenz and Howe 2007). The presence of divalent metals (Mn^{2+}, Zn^{2+}, Mg^{2+}, Ca^{2+}, Cu^{2+}) within the brain have various functions such as activation of glutamate receptors, synaptic transmission, cellular signaling, and can act as cofactors for different enzymes within the brain (Marchetti 2014; Szewczyk 2013; Takeda 2003). BMAA is also a known chelator of divalent metals; it is essential to understand how BMAA affects the natural metal equilibria present in the brain (Nunn and O'Brien 1989). Of particular interest are the emerging roles of zinc, copper, and magnesium in maintaining basal brain homeostasis, as well as regulating the neurodegenerative hallmarks associated with each neurological disease (Barnham and Bush 2014; Hozumi et al. 2011). Under excitotoxic conditions or even irregular potentiation, free ionic metals such as Zn^{2+} are released in high nanomolar concentrations causing perturbations in the hippocampus (Frederickson et al. 2004).

Similarly, NMDA activation causes synaptosomes to release Cu^{2+} into the synapse, causing an accumulation of Cu^{2+} within the neuronal environment (Barnham and Bush 2014; Hartter and Barnea 1988). The accumulation of Cu^{2+} has been shown to inhibit ionotropic receptors and suppress long-term potentiation in rat hippocampal slices (Doreulee et al. 1997; Trombley and Shepherd 1996; Weiser and Wienrich 1996). Both Zn^{2+} and Cu^{2+} can bind to amyloid precursor proteins (APP) and amyloid-beta (Aβ), causing aggregation of amyloid plaques (Barnham and Bush 2014). BMAA has a backbone similar to ethylenediamine, and BMAA is purported to exhibit similar affinity to specific transition metals such as Fe^{2+}, Ni^{2+}, Cu^{2+}, Zn^{2+}, and Co^{2+}. Studies by Nunn et al. (Nunn et al. 1989) showed that Zn^{2+}BMAA and synthesized Cu^{2+}-BMAA structures were relatively stable in solution. The results from Zimmerman et al. established that BMAA and its adducts coexist, and it is essential to understand if divalent metal ions bind to BMAA or its adducts (Zimmerman et al. 2016). More importantly, how the BMAA-metal interactions alter the kinetic equilibria between the BMAA and the carbamate adducts.

The Zimmerman et al. study investigated in detail how the affinity of specific divalent metals (Mg^{2+}, Zn^{2+}, and Cu^{2+}) disrupts the dynamic equilibria of carbamate formation of BMAA (Zimmerman et al. 2016). The equilibrium constants of BMAA and its carbamate adducts were determined using two-dimensional chemical exchange spectroscopy (EXSY) as a function of ion concentrations, accompanied by a detailed accounting of the various equilibrium processes. Additional experiments using circular dichroism and UV-Vis spectroscopy were performed to validate the NMR results. Our results show that BMAA differentially interacts with divalent metals as determined by the NMR spectral changes with Cu^{2+} showing the most notable effect followed by Zn^{2+} and finally Mg^{2+} with the least change. The ability of BMAA to preferentially interact with one divalent ion versus another under physiological conditions can significantly alter the relative levels of BMAA and its carbamate species. Alterations in the dynamic equilibria of BMAA in the presence of

divalent metals can provide a better understanding as to the function of BMAA as a neurotoxic molecule.

Materials and Methods

Sample Conditions

Stock solutions of BMAA (50 mM), $NaHCO_3$ (500 mM), $CuCl_2$ (200 mM), $ZnCl_2$ (200 mM) and $MgCl_2$ (200 mM) were prepared in D_2O. A solution of BMAA to $NaHCO_3$ (1:20; 10 mM BMAA and 200 mM $NaHCO_3$) was prepared in D_2O containing 3-(Trimethylsilyl) propionic-2, 2, 3, 3-d4 acid sodium salt (1 mM, TSP) as a reference in the NMR experiments. Individual BMAA-metal solutions were prepared as follows: a 1:20 solution of BMAA to $NaHCO_3$ was titrated with 0.5 mM, 1 mM, 2 mM, 3 mM, 4 mM, and 5 mM of each metal. The pH of all NMR samples was measured using a Mettler Toledo pH meter with a microelectrode (3 mm diameter) and adjusted to a physiological pH of 7.4 using deuterium chloride (DCl). All NMR samples (600 μl) were freshly prepared before each experiment.

Circular Dichroism Spectroscopy

Circular Dichroism (CD) experiments were performed using a Jasco CD spectrometer using standing operating procedures. The sample conditions (e.g., pH and BMAA: HCO_3) for the CD experiments were the same as the NMR experiments.

NMR Experiments

All the NMR experiments were performed on a 400 MHz VNMRS spectrometer (Varian-Agilent) at a probe temperature of 30 °C. The experimental parameters were described previously (Zimmerman et al. 2016). One-dimensional NMR spectra of freshly prepared samples were performed before and after running the 2D EXSY experiments to confirm that the sample conditions were unaltered during the data collection. The spectra were processed and analyzed using Mestrenova (Mestrelab Research, Santiago de Compostela, Spain).

Analysis of EXSY and Determination of Equilibrium Constants

The complete details of the study of chemical equilibria of carbamate adducts formation are described previously (Zimmerman et al. 2016). Herein, for the sake of completion, an overview of the mechanism for analysis of the chemical equilibria process between BMMA and its primary (α) and secondary (β) carbamates and subsequent interaction with the divalent metals is presented. The pre-formation of HCO_3^- and aqueous CO_2, at pH ~7.4 is shown by the red dashed arrows of Fig. 1. The aqueous CO_2, which reacts subsequently with the α- and β-amines of BMAA to form the respective α-BMAA (blue arrows) and β-BMAA carbamates (red arrows).

Following the chemical exchange process for nuclear spin relaxation between the three spins (I=½), the rate constants of magnetization exchange that are related to the chemical kinetics can be estimated using well-established methods (Jeener et al. 1979; Mcconnell 1958; Meier and Ernst 1979). Using the total concentration of BMAA determined upon integrating the NMR signals from the 1D proton (^1H) experiments and estimations of the total

concentration of carbon dioxide using the equilibration process of carbamate and carbamic acid (Fig 3), the quasi-equilibrium kinetics of BMAA and its carbamates for a given sample conditions (BMAA:HCO_3^- concentration) can be estimated (Zimmerman et al. 2016). The concentrations of $[BMAA]_T$, [α-carbamate] and [β-carbamate], were obtained from the integration of the 1D ^1H spectra (total BMAA concentration = $[BMAA]_T$, or [α-carbamate] or [β-carbamate]). The concentration of BMAA (unprotonated) was calculated using the known pK_a of amines (Arnold et al. 1969). This was assuming that the pK_a for the primary and secondary amines were the same, temperature independent, and the total carbon dioxide concentration was estimated using the total $NaHCO_3$ in the solution (pK_{a1} of H_2CO_3 =6.34) (Dean 1992). At the neutral pH, the ratios $[H_2CO_3]/[CO_2]$ and $[H_2CO_3]/[HCO_3^-]$ are small (< 0.005 or less) (Gibbons and Edsall 1963). Upon substituting these values and the corresponding rate constants determined from the EXSY spectrum, the equilibrium constants can be determined.

In continuing the equilibrium processes to include the interaction with divalent metal ions (Fig 1), we assume the framework defined above is considered valid under two conditions; first, the reaction equilibrium between the BMAA (or the adducts) with metal ions is much faster than the BMAA equilibrium with the carbamates, and secondly, the divalent metal ions do not directly interact with other species in the solution. These assumptions lead to the fact that any change in the estimated equilibrium constant (K_α^* and K_β^*) can directly be related to the amount of either the reactants or products (BMAA or adducts) as defined by the law of mass action.

Uncertainty in the measured values was determined by an error propagation method (using R Statistical environment). The standard deviation in the spectral data was measured by estimating the noise in the 1D or 2D data by randomly selecting five different regions of the spectra. The standard deviation in each of the measured values and the error propagation were determined using a *Monte Carlo* method based on the generation of a large number of sampling (~5,000) with reference to the mean and standard deviation of the individual variables in the experimental measurements. Typically, the accuracy of the measured peak intensity in the 1D spectra is ~1%, and the variation in the diagonal and cross peak volumes of the 2D data is in the range of 3–7%.

Results

Chemical Structure and Relative Population Changes with Increasing Metal Ion Concentrations

Any changes in the chemical shift of the protons can be directly related to chemical structural changes. The methyl region of the NMR spectra of BMAA and its carbamate adducts (BMAA concentration of 10 mM and BMAA: HCO_3^- of 1:20) acquired as a function of increasing concentration of metal ions, are shown in Fig. 2. Fig. 3 (panels a, b, c) show the changes in the chemical shifts for the methyl resonances of BMAA (B, black circles), α-BMAA (α, blue squares), and β-BMAA (β, red diamonds) with increasing concentrations of Mg^{2+}, Zn^{2+}, and Cu^{2+}. The bottom row of Fig. 3 shows the estimated changes in the population of BMAA (B, black circles), α-BMAA (α blue squares), and β-BMAA (β, red diamonds) as a function of the concentration of Mg^{2+} (d), Zn^{2+} (e) and Cu^{2+}

(f). In the absence of metal ions, the chemical shifts of the BMAA (2.74 ppm), α–BMAA (2.77 ppm), and β-BMAA (2.86 ppm) are observed (see Figure S1). The corresponding populations of the BMAA (19.7%), α–BMAA (50.1%), and β-BMAA (30.2%) were estimated from the spectra peak area. Though the chemical shifts of the resonances are independent of the BMAA: HCO_3^- ratio, the populations are dependent on the HCO_3^- concentration, which is characteristic of a quasi-equilibrium process (Diaz-Parga et al. 2018; Zimmerman et al. 2016).

The chemical shifts of the methyl protons of BMAA, α–BMAA, and β-BMAA remain unaltered, with increasing Mg^{2+} concentration (Fig. 3a). However, the population of BMAA, α–BMAA and β-BMAA are altered; BMAA increases (20% to 41%), while α–BMAA (50% to 44%) and β-BMAA (30% to 15%) are reduced by 6% and 15 %(Fig. 3d). The estimated coefficient of variation on the populations is <5%. In the assay of increasing Mg^{2+} concentration, the BMAA increases by ~20%, while the adducts concentration decreases accordingly. As a chemical shift change is a general indication of structural change, the lack of chemical shift changes on BMAA and its adducts suggest that Mg^{2+} interacts weakly with all three species (Fig. 3a) simultaneously. The spectral features of the other protons also remain unchanged in the presence of Mg^{2+} (Fig. S2).

In contrast to magnesium ions, the interaction of BMAA-carbamate with zinc ions are more prominent, demonstrated by both the chemical shift (Fig 3b) and population changes (Fig. 3e). With increasing Zn^{2+} concentration, the chemical shifts of the α-BMAA and β-BMAA do not change, the methyl chemical shift of BMAA is up-field by 0.23 ppm. The notable change in the resonance frequency is a clear indication of zinc atoms coordinating preferentially with BMAA, and not with the α– or β–carbamates. The significant difference in the chemical shift of BMAA correlates with an increase in the BMAA: Zn^{2+} complex. The population of BMAA without zinc doubles with 0.5 mM Zn^{2+} (from 20% to 46%) and increases to 74% with 5 mM of zinc. With relatively little changes in the chemical shifts of the α- and β- carbamates of BMAA (Fig 2b), the formation of BMAA: Zn^{2+} complexes are favored by altering the dynamic equilibria between the BMAA and its adducts. It is important to note that Zn^{2+} complexes with BMAA were only found in the presence of bicarbonate (here at 1:20 ratio), and no noticeable spectral changes were observed when Zn^{2+} was added to free BMAA (Figure S3). The effect of BMAA: Zn^{2+} formation is also seen in the other protons of BMAA (Fig S2).

Proton NMR spectroscopy is not considered a viable option to characterize paramagnetic copper (II) complexes, because the slow electronic relaxation leads to broad resonances (Bertini et al. 1993). Fig. S3 shows broadened resonances in the presence of Cu^{2+} (2 mM) with BMAA. However, the spectral resolution at 400 MHz is adequate to resolve the BMAA and its carbamate at low concentrations of Cu^{2+} (Fig. 2c). The resonances of all the BMAA species shift downfield even at low concentrations of Cu^{2+}. The chemical shift on the methyl protons of BMAA is less (0.03 ppm) in comparison with the shifts on the α-BMAA and β-BMAA (~0.1 ppm). As in the case of BMAA: HCO_3^- solution interacting with zinc ions, the population of the BMAA increased with increasing Cu^{2+} (Fig. 3f), and the corresponding α-BMAA and β-BMAA populations decreased. Both α-BMAA and β-BMAA reduced (~25%) in their respective populations, with an increase (~48%) in the

population of BMAA (Fig. 2f). These estimates are approximate due to the increased linewidths of all the resonances, and at higher concentrations of Cu^{2+}, it is not possible to integrate the peak areas. Even with the limited data (four concentrations of Cu^{2+}), the trend suggests that the interaction of BMAA shows the most changes with Cu^{2+} even with the limited complex formation with the carbamate adducts.

EXSY Data and Determination of Equilibrium Parameters

The chemical shifts indicate structural changes induced by the divalent metals to the BMAA and its carbamate adducts, while the population estimates provide the relative changes in the total amount due to dynamic equilibria of the various species. Two-dimensional EXSY based approach allows to quantitatively determine the equilibrium constants involved in the process (Fig. 1). As demonstrated previously under physiological conditions, BMAA exists in a dynamic equilibrium between free, and the α- and β- carbamate forms (Zimmerman et al. 2016). The two-dimensional EXSY data combined with the relaxation matrix analysis can estimate the dynamic parameters involved between all three species.

Increasing the concentration of Mg^{2+} has a minimal effect on the on the dynamic equilibria between the BMAA and it is carbamates. Figure S4 (Panels a-f) shows the EXSY spectra of the BMAA-bicarbonate solution with increasing concentrations of $Mg2^{+}$. The various equilibrium parameters estimated from the EXSY spectra using the relaxation matrix approach are listed in Table S1. For comparison, Table S1 also contains the equilibrium parameters estimated in the absence of metal ions. In the absence of metal ions, the equilibrium constants (K_α and $K_\beta \times 10^6$) for the formation of α- and β-carbamates are 13.35 ± 1.69 and 3.19 ± 0.08, respectively. The addition of Mg^{2+} does not alter these equilibrium constants significantly; 13.78 ± 3.96 and 1.30 ± 0.12, for the formation of α- and β-carbamate forms, respectively. The combination of results from the chemical shift changes (Fig. 3a), relative population changes (Fig. 3d) and the dynamic equilibria (Fig S4 and Table S1) suggest that the complexes of Mg^{2+}: BMAA and Mg^{2+}:(α-carbamate/β-carbamate) in solution are weakly bound by ionic forces. The weak ionic interactions between the electronegative atoms nitrogen and oxygen cause small perturbations in the equilibria giving rise to different populations of BMAA, α-carbamate, and β-carbamate in solution. However, because the complexes are weakly bound, they can interconvert back and forth between their respective species readily. As a result, in the presence of Mg^{2+}, the dynamic equilibria that exists between BMAA, α-carbamate, and β-carbamate can adjust to the presence of Mg^{2+} by causing alterations to the availability and kinetic rate of formation for BMAA, α-carbamate, and β-carbamate.

The complexation of BMAA with Zn^{2+} is relatively stronger than its ability to produce the α-carbamate and β-carbamate species, as evidenced by the increase in the population BMAA with increasing Zn^{2+} concentration (Fig. 3b and Fig. 3e).

The EXSY spectra as a function of increasing Zn^{2+} concentration are shown in Figure 4, and the estimated dynamic equilibrium parameters are listed in Table S1. Analysis of the 2D EXSY spectrum produces kinetic data that suggests the emergence of new dynamic equilibria different from the one observed in the 1:20 BMAA: $NaHCO_3$ solution. In comparison to the 1:20 BMAA: HCO_3-, the presence of Zn^{2+} causes a significant decrease

in the rate of formation for the α-carbamate ($k_{1\alpha}$*) and the β-carbamate ($k_{1\beta}$*). The second-order rate constant ($k_{1\alpha}$*, $k_{1\beta}$*) for the rate of formation of α-carbamate ranges from 1.15±0.07 $M^{-1}s^{-1}$ to 0.30±0.06 $M^{-1}s^{-1}$ while the β-carbamate ranges from 4.79±0.10 $M^{-1}s^{-1}$ to 1.36±0.09 $M^{-1}s^{-1}$. While the rate of decomposition for $k_{2\alpha}$* and $k_{2\beta}$* are within the range of 0.11±0.01 s^{-1} to 0.71±0.00 s^{-1} and 1.47±0.01 s^{-1} to 3.81±0.00 s^{-1} for the α-carbamate and β-carbamate, (Table S1). In the presence of Zn^{2+}, the rate of formation constants ($k_{1\alpha}$ and $k_{1\beta}$*) notably decreased while the rates of decompositions ($k_{2\alpha}$* and $k_{2\beta}$*) are relatively the same. Meaning that the dynamic equilibria are shifted towards the formation of BMAA because Zn^{2+} is sequestering BMAA from the system. As seen in Figure 5, the equilibrium constants (K_i*) for the formation of α-carbamate and β-carbamate species decrease with increasing amounts of Zn^{2+}. At a stoichiometric ratio of 1:1 (BMAA: Zn^{2+}), the equilibrium constants for forming both α-carbamate and β-carbamates are similar (1.07 ± 0.21 M^{-1} and 0.55 ± 0.04 M^{-1}, respectively) due to the ability of selective formation of BMAA: Zn^{2+} complexes. The rapidly decreasing of K_i* correlates with the propensity of the dynamic equilibria to favor the formation of the reactants (BMAA), as opposed to the products (α-carbamate and β-carbamate) in solution.

EXSY experiments performed in the presence of Cu^{2+} were not used for extracting equilibrium parameters due to line broadening and lack of resolution in the spectra. However, evidence for BMAA complexation with copper ions is seen with the CD and UV-vis spectra (see results related to Fig. 6 below).

Evidence of complex formation from other spectroscopic techniques: CD and UV-Visible Spectra

Conformational changes in a protein-metal complex can be studied based on the circular dichroism (CD) absorption spectra (Tsangaris and Martin 1970). CD detects the presence of n →π electron interactions between the electrons on the free p-orbital on nitrogen and the overlapping π orbitals present on the carbonyl double bond. CD spectra of BMAA at the same experimental conditions as the NMR spectroscopic studies are summarized in Figure 6. Absorption of circularly plane-polarized light by this interaction is typically seen between 210 −220 nm, as seen in the 1:20 BMAA (Figure 6a) in a $NaHCO_3$ solution containing the carbamate species (Figure 6). The CD spectra of free BMAA (dashed lines) show a significantly different spectral signature than the 1:20 BMAA: $NaHCO_3$ solution (dotted lines). In the presence of BMAA, the chirality of the α-carbon caused a higher absorbance producing a positive spectrum (dashed lines). However, the addition of carbamic acid (-NH_2COOH), to either the α-amine or β-amine of BMAA, causes the carbamate species to absorb differentially producing a spectrum between 210 nm to 220 nm, due to the interference of the newly added n → π interaction. Increasing the Mg^{2+} concentrations does not alter the CD spectra significantly (Fig 6a, dotted lines vs. continuous colored lines), suggesting that Mg^{2+} does not alter the chiral carbon dichroism.

The effect of Zn^{2+} interactions with the BMAA: HCO_3− (1:20) solution on the CD spectra are shown in Fig 6b. The ability of circular dichroism to detect the interaction between the –NH_2 group and the –COOH functional group (n→π) is useful in providing qualitative data regarding the presence of carbamate species in solution. In comparison, the 1:20 BMAA:

$NaHCO_3$ solution produces the typical n→π interaction due to the presence of carbamate products in solution. The decrease in the n→π absorption shown in Fig 6b, with increasing concentrations of Zn^{2+}, correlates with an increase in the BMAA population in solution. The Zn-NH_2 complexes formed to prevent the HCO_3^- from interacting with either the α-amine or the β-amine. This results in a gradual decrease in the absorption of the n→π electrons from the nitrogen electrons and the carbonyl electrons. Loss of absorption occurs at 2 mM of Zn^{2+} when the population of BMAA exceeds the population of carbamylated species (60% vs. 40%) (Fig 6b). The loss of absorption indicates an increase in the population of BMAA.

The effect of Cu^{2+} interaction with BMAA: HCO_3^- has more substantial changes in the CD spectral changes in comparison with that of Zn^{2+} interactions (Fig 6c). More considerable spectral changes in the 210–220 nm range indicate the formation of BMAA: Cu^{2+} complexes more effectively in the solution. Additional UV-vis data to demonstrate the binding of Cu^{2+} to the BMAA: HCO_3^- is shown in the supporting material (Fig S5). In the absence of Cu^{2+}, the BMAA: HCO_3^- solution is spectroscopically silent. In the absence of BMAA, a solution of 200 mM HCO_3^- and $Cu^{2+,}$ the absorption occurs at a λ_{max} of 850 nm, corresponding to free Cu^{2+}. In the presence of BMAA, Cu^{2+} causes the λ_{max} to change to ~560 nm, indicating a BMAACu^{2+} complex. Increasing the amount of Cu^{2+} increases the intensity of the absorption band, suggesting the formation of a Cu^{2+} :(BMAA) $_n$ structure (Fig S5).

Discussion

BMAA is a small molecule (118.14 g/mol), its structure contains three electronegative atoms, and in the carbamylated form, additional oxygen atoms are a part of the structure. The presence of multiple electronegative nitrogen atoms and additional oxygen atoms allows for possible interactions with the divalent metal Mg^{2+}. Mg^{2+} is a necessary regulator of ionotropic receptors located within the hippocampus; BMAA: Mg^{2+} interactions can interrupt the natural Mg^{2+} homeostasis within the brain (Traynelis et al. 2010). Because Mg^{2+} is a small, non-polarizable cation, it has minimal interactions with Lewis bases (e.g., fluorine, oxygen, and nitrogen) (Pearson 1963). Though the chemical shift changes in the NMR spectra are minimal in the presence of Mg^{2+}, the slight shifts in the relative populations of the three species observed (Fig. 3) are indicative of the possible weak ionic interaction between BMAA and its carbamates with magnesium ions.

In comparison to a 1:20 BMAA: $NaHCO_3$, the methyl resonances of BMAA and α-carbamate are shifted downfield by ~0.02 ppm and 0.01 ppm in the presence of Mg^{2+}, with no significant shifts seen in the β-carbamate methyl resonance (< 0.01 ppm). The de-shielding effect observed is most likely due to the interaction of Mg^{2+} with at least one of the oxygen atoms on the carboxylate group, causing a downfield shift in the spectra containing Mg^{2+} (Kondo et al. 1984). Oddly, the presence of carboxylic groups on BMAA and its species would suggest Mg^{2+} preferentially binds to the α-carbamate and β-carbamate species, due to the increase in the number of oxygen atoms in the structure. Instead, the Mg^{2+}-β-carbamate interaction is almost non-existent as there is no noticeable shift in comparison to the β-carbamate methyl resonance, seen in the 1:20 BMAA: $NaHCO_3$ (Figs

2, Fig 3). Gradual increases in the concentration of Mg^{2+} did not produce any notable changes in the chemical shifts or intensities in the NMR spectra (data not shown).

BMAA in the absence of HCO_3^- did not interact with zinc (Fig. S3). In the absence of HCO_3^-, the solution of 10 mM free BMAA has a pH of ~6 compared to the pH of BMAA in the presence of HCO_3^- (pH 7.4). The pH of the solution must be higher than the pKa of the α-amine (pKa 6.63) for the formation of the Zn^{2+} :(BMAA) $_2$ complexes. Because Zn-NH_2 formation is not a concerted reaction, the basicity of the solution must first increase to deprotonate the charged α-amine (NH_3^+) (Krężel and Maret 2016). Deprotonation of the amine in basic conditions expedites the rate of formation of the Zn-NH_2 interaction (Krężel and Maret 2016). Zn-BMAA complexes show an apparent upfield shift in comparison to a 1D spectrum of free BMAA methyl resonance, in agreement with the literature (Glover et al. 2012). The upfield shift, corresponding to the BMAA methyl resonance, is caused by a conformational change in the structure of BMAA. The formation of Zn^{2+}:$(BMAA)_2$ complexes shields the nucleus from the external magnetic field, causing it to resonate at a different frequency (Fig 2b). Also, the relative population of the methyl resonances is increased in comparison to the 1:20 BMAA: $NaHCO_3$ solution (Fig 3b and Fig 3e). As the concentration of Zn^{2+} increased, the intensity of the BMAA methyl resonance also increased, while the intensities of the αcarbamate and β-carbamate decreased. The Zn-NH_2 interactions prevent HCO_3^- from interacting with the α- and β-amine, causing equilibria to favor the formation of BMAA.

Utilization of biophysical methods: circular dichroism, UV-Vis, and NMR have revealed that BMAA has a high affinity for the transition metals Zn^{2+} and Cu^{2+} in comparison to Mg^{2+}. The presence of Mg^{2+} did not produce significant alterations in the chemical equilibria between BMAA and its carbamate species. Spectroscopic studies of zinc suggest that Zn^{2+} interacts with BMAA and alters the chemical equilibria of BMAA and its carbamates. Both structural (chemical shifts) and relative populations (intensity of peaks) along with an estimation of equilibrium constants suggest the formation of BMAA: Zn^{2+} complexes in bicarbonate solutions. Further evidence using the CD data demonstrates relative changes in the dichroism in the 210–220 nm range. The formation of the carbamic acid functional group introduces an n→π transition that arises from the interaction between the electrons on the free p-orbital of nitrogen and the overlapping π orbitals present on the carbonyl double bond. Though Cu^{2+} tends to form complexes similar to Zn^{2+}, NMR results are limited due to line broadening and a lack of resolution. However, the CD and UV-vis data support the formation of BMAA: Cu^{2+} complex causing alterations in the equilibria of BMAA and its carbamate adducts. The results from NMR, UV-Vis, and circular dichroism demonstrate that BMAA equilibria are significantly altered in the presence of Cu^{2+} and Zn^{2+} but not in the presence of Mg^{2+}.

Conclusion

The investigation into the chelating abilities of BMAA and its carbamates has revealed that in the presence of divalent metals, BMAA can sequester divalent metals, to varying degrees ($Mg^{2+} < Zn^{2+} < Cu^{2+}$) causing a change in the dynamic equilibria between BMAA and its carbamates. BMAA is a known chelator of Cu^{2+}, Zn^{2+}, and Ni^{2+}, suggesting the potential

for BMAA to bind to these divalent metals (Nunn and O'Brien 1989). Glover et al. examined the role of BMAA binding to zinc using mass spectrometry (Glover et al. 2012). Detailed mass spectroscopic investigation in combination with NMR and preliminary computational modeling suggests a possible distorted tetrahedral geometry of coordination though it was not possible to unambiguously determine the conformation of the $Zn(BMAA)_2$ complex (Glover et al. 2012). Presumably, Zn^{2+} can coordinate with BMAA resulting in the formation of a $Zn(BMAA)_2$ complex, similar to that of $Cu(BMAA)_2$, to form a four-coordinate complex in which each amino acid binds through both N atoms (Nunn and O'Brien 1989). The experiments conducted provide further insight into the ability of BMAA to chelate Zn^{2+}, thus, leading to a potential transport mechanism of BMAA and a second pathway for other neurodegenerative effects on metal-binding enzymes (copper-zinc superoxide dismutase).

The equilibria established by Zimmerman et al. (Zimmerman et al. 2016) shows that the population of BMAA in solution is roughly 30%. However, in the presence of Zn^{2+} (and Cu^{2+}), the population of BMAA is increased in solution. Although no quantifiable data were obtained for Cu^{2+}, it is presumed that the BMAA: Cu^{2+} interactions also increases the population of BMAA in solution. The production of coordinated BMAA metal complexes causes an increase in the population of BMAA and decreases the population of both carbamate species in solution. As proposed by Weiss and Choi, the neurotoxic properties of BMAA are thought to be mediated primarily by the presence of the carbamate adducts, specifically the β-carbamate (Weiss 1988). The data obtained, however, suggest that BMAA may affect neuronal regulatory processes through multiple modes of action, either through direct means: production of β-carbamate or subsequent interactions, such as metal dysregulation.

Supplementary Material

Refer to Web version on PubMed Central for supplementary material.

Acknowledgments

PD acknowledges the support of the Bridges to Doctorate Program (R25 GM115293). The authors thank C. Cortney for the critical reading of the manuscript.

References

Arnold H, Pahls K, Potsch D (1969) Reaktion von N-(Chloräthyl)-2-oxazolidon mit primären Aminen Tetrahedron Letters 10:137–139 doi:10.1016/s0040-4039(01)87492-x

Barnham KJ, Bush AI (2014) Biological metals and metal-targeting compounds in major neurodegenerative diseases Chem Soc Rev 43:6727–6749 doi:10.1039/c4cs00138a [PubMed: 25099276]

Bertini I, Turano P, Vila AJ (1993) Nuclear magnetic resonance of paramagnetic metalloproteins Chemical reviews 93:2833–2932 doi:10.1021/cr00024a009

Bradley WG, Cox PA (2009) Beyond Guam: cyanobacteria, BMAA and sporadic amyotrophic lateral sclerosis. Taylor & Francis,

Bradley WG, Mash DC (2009) Beyond Guam: the cyanobacteria/BMAA hypothesis of the cause of ALS and other neurodegenerative diseases Amyotrophic lateral sclerosis : official publication of the

World Federation of Neurology Research Group on Motor Neuron Diseases 10 Suppl 2:7–20 doi:10.3109/17482960903286009

Brand LE, Pablo J, Compton A, Hammerschlag N, Mash DC (2010) Cyanobacterial blooms and the occurrence of the neurotoxin, beta-N-methylamino-l-alanine (BMAA), in South Florida aquatic food webs Harmful Algae 9:620–635 doi:10.1016/j.hal.2010.05.002 [PubMed: 21057660]

Buenz EJ, Howe CL (2007) Beta-methylamino-alanine (BMAA) injures hippocampal neurons in vivo Neurotoxicology 28:702–704 doi:10.1016/j.neuro.2007.02.010 [PubMed: 17379313]

Chiu AS, Gehringer MM, Braidy N, Guillemin GJ, Welch JH, Neilan BA (2012) Excitotoxic potential of the cyanotoxin beta-methyl-amino-L-alanine (BMAA) in primary human neurons Toxicon : official journal of the International Society on Toxinology 60:1159–1165 doi:10.1016/j.toxicon.2012.07.169 [PubMed: 22885173]

Chiu AS, Gehringer MM, Braidy N, Guillemin GJ, Welch JH, Neilan BA (2013) Gliotoxicity of the cyanotoxin, beta-methyl-amino-L-alanine (BMAA) Scientific reports 3:1482 doi:10.1038/srep01482 [PubMed: 23508043]

Chiu AS, Gehringer MM, Welch JH, Neilan BA (2011) Does alpha-amino-beta-methylaminopropionic acid (BMAA) play a role in neurodegeneration? International journal of environmental research and public health 8:3728–3746 doi:10.3390/ijerph8093728 [PubMed: 22016712]

Choi DW (1988) Glutamate neurotoxicity and diseases of the nervous system Neuron 1:623–634 [PubMed: 2908446]

Cox PA et al. (2005) Diverse taxa of cyanobacteria produce beta-N-methylamino-L-alanine, a neurotoxic amino acid Proceedings of the National Academy of Sciences of the United States of America 102:5074–5078 doi:10.1073/pnas.0501526102 [PubMed: 15809446]

Davis AJ, Obrien P, Nunn PB (1993) Studies of the Stability of Some Amino-Acid Carbamates in Neutral Aqueous-Solution Bioorganic Chemistry 21:309–318 doi:DOI 10.1006/bioo.1993.1026

Dean JA (1992) Lange's Handbook of Chemistry. 14th edn. McGraw-Hill, Inc, New York, USA.

Diaz-Parga P, Goto JJ, Krishnan VV (2018) Chemistry and Chemical Equilibrium Dynamics of BMAA and Its Carbamate Adducts Neurotox Res 33:76–86 doi:10.1007/s12640-0179801-2 [PubMed: 28921378]

Doreulee N, Yanovsky Y, Haas HL (1997) Suppression of long-term potentiation in hippocampal slices by copper Hippocampus 7:666–669 doi:10.1002/(SICI)1098-1063(1997)7:6<666::AID-HIPO8>3.0.CO;2-C [PubMed: 9443062]

Frederickson CJ, Maret W, Cuajungco MP (2004) Zinc and excitotoxic brain injury: a new model Neuroscientist 10:18–25 doi:10.1177/1073858403255840 [PubMed: 14987444]

Gibbons BH, Edsall JT (1963) Rate of Hydration of Carbon Dioxide and Dehydration of Carbonic Acid at 25 Degrees J Biol Chem 238:3502–3507 [PubMed: 14085409]

Glover WB, Liberto CM, McNeil WS, Banack SA, Shipley PR, Murch SJ (2012) Reactivity of beta-methylamino-L-alanine in complex sample matrixes complicating detection and quantification by mass spectrometry Analytical chemistry 84:7946–7953 doi:10.1021/ac301691r [PubMed: 22905767]

Hartter DE, Barnea A (1988) Evidence for release of copper in the brain: depolarization-induced release of newly taken-up 67copper Synapse 2:412–415 doi:10.1002/syn.890020408 [PubMed: 3187909]

Hozumi I et al. (2011) Patterns of levels of biological metals in CSF differ among neurodegenerative diseases Journal of the Neurological Sciences 303:95–99 doi:10.1016/j.jns.2011.01.003 [PubMed: 21292280]

Jeener J, Meier B, Bachmann P, Ernst R (1979) Investigation of exchange processes by two-dimensional NMR spectroscopy The Journal of chemical physics 71:4546–4553

Jonasson S et al. (2010) Transfer of a cyanobacterial neurotoxin within a temperate aquatic ecosystem suggests pathways for human exposure Proceedings of the National Academy of Sciences of the United States of America 107:9252–9257 doi:10.1073/pnas.0914417107 [PubMed: 20439734]

Kondo H, Miura K, Uno S, Sunamoto J (1984) Proton nmr study of metal coordination to biotin derivatives Journal of Inorganic Biochemistry 21:93–102 doi:10.1016/0162-0134(84)85042-4

Krężel A, Maret W (2016) The biological inorganic chemistry of zinc ions Archives of biochemistry and biophysics 611:3–19 [PubMed: 27117234]

Lobner D, Piana PM, Salous AK, Peoples RW (2007) Beta-N-methylamino-L-alanine enhances neurotoxicity through multiple mechanisms Neurobiology of disease 25:360–366 doi:10.1016/j.nbd.2006.10.002 [PubMed: 17098435]

Marchetti C (2014) Interaction of metal ions with neurotransmitter receptors and potential role in neurodiseases Biometals 27:1097–1113 doi:10.1007/s10534-014-9791-y [PubMed: 25224737]

Mcconnell HM (1958) Reaction Rates by Nuclear Magnetic Resonance Journal of Chemical Physics 28:430–431 doi:Doi 10.1063/1.1744152

Meier BH, Ernst RR (1979) Elucidation of chemical exchange networks by two-dimensional NMR spectroscopy: the heptamethylbenzenonium ion Journal of the American Chemical Society 101:6441–6442 doi:10.1021/ja00515a053

Murch SJ, Cox PA, Banack SA (2004a) A mechanism for slow release of biomagnified cyanobacterial neurotoxins and neurodegenerative disease in Guam Proceedings of the National Academy of Sciences of the United States of America 101:12228–12231 doi:10.1073/pnas.0404926101 [PubMed: 15295100]

Murch SJ, Cox PA, Banack SA, Steele JC, Sacks OW (2004b) Occurrence of beta-methylamino-l-alanine (BMAA) in ALS/PDC patients from Guam Acta neurologica Scandinavica 110:267–269 doi:10.1111/j.1600-0404.2004.00320.x [PubMed: 15355492]

Myers TG, Nelson SD (1990) Neuroactive carbamate adducts of beta-N-methylamino-L-alanine and ethylenediamine. Detection and quantitation under physiological conditions by 13C NMR J Biol Chem 265:10193–10195 [PubMed: 2113048]

Nunn PB, O'Brien P (1989) The interaction of beta-N-methylamino-L-alanine with bicarbonate: an 1H-NMR study FEBS letters 251:31–35 [PubMed: 2666171]

Nunn PB, O'Brien P, Pettit LD, Pyburn SI (1989) Complexes of zinc, copper, and nickel with the nonprotein amino acid L-α-amino-β-methylaminopropionic acid: A naturally occurring neurotoxin Journal of Inorganic Biochemistry 37:175–183 doi:10.1016/01620134(89)80040-6 [PubMed: 2600597]

Pablo J et al. (2009) Cyanobacterial neurotoxin BMAA in ALS and Alzheimer's disease Acta neurologica Scandinavica 120:216–225

Pearson RG (1963) Hard and Soft Acids and Bases Journal of the American Chemical Society 85:3533-& doi:DOI 10.1021/ja00905a001

Richter KE, Mena EE (1989) L-beta-methylaminoalanine inhibits [3H]glutamate binding in the presence of bicarbonate ions Brain research 492:385–388 [PubMed: 2568879]

Smith QR, Nagura H, Takada Y, Duncan MW (1992) Facilitated transport of the neurotoxin, β-N-methylamino-L-alanine, across the blood-brain barrier Journal of neurochemistry 58:1330–1337 [PubMed: 1548467]

Szewczyk B (2013) Zinc homeostasis and neurodegenerative disorders Front Aging Neurosci 5:33 doi:10.3389/fnagi.2013.00033 [PubMed: 23882214]

Takeda A (2003) Manganese action in brain function Brain Res Brain Res Rev 41:79–87 [PubMed: 12505649]

Traynelis SF et al. (2010) Glutamate Receptor Ion Channels: Structure, Regulation, and Function Pharmacological Reviews 62:405–496 doi:10.1124/pr.109.002451 [PubMed: 20716669]

Trombley PQ, Shepherd GM (1996) Differential modulation by zinc and copper of amino acid receptors from rat olfactory bulb neurons J Neurophysiol 76:2536–2546 doi:10.1152/jn.1996.76.4.2536 [PubMed: 8899625]

Tsangaris JM, Martin RB (1970) Visible circular dichroism of copper(II) complexes of amino acids and peptides J Am Chem Soc 92:4255–4260 [PubMed: 5428384]

Vega A (1967) α-Amino-β-methylaminopropionic acid, a new amino acid from seeds of Cycas circinalis Phytochemistry 6:759–762 doi:10.1016/s0031-9422(00)86018-5

Weiser T, Wienrich M (1996) The effects of copper ions on glutamate receptors in cultured rat cortical neurons Brain research 742:211–218 [PubMed: 9117397]

Weiss JC D (1988) Beta-N-methylamino-L-alanine neurotoxicity: requirement for bicarbonate as a cofactor. Science 241:973–975 [PubMed: 3136549]

Weiss JH, Choi DW (1988) Beta-N-Methylamino-L-Alanine Neurotoxicity - Requirement for Bicarbonate as a Cofactor Science 241:973–975 doi:DOI 10.1126/science.3136549 [PubMed: 3136549]

Xie X, Basile M, Mash DC (2013) Cerebral uptake and protein incorporation of cyanobacterial toxin beta-N-methylamino-L-alanine Neuroreport 24:779–784 doi:10.1097/WNR.0b013e328363fd89 [PubMed: 23979257]

Zimmerman D, Goto JJ, Krishnan VV (2016) Equilibrium Dynamics of beta-N-Methylamino-LAlanine (BMAA) and Its Carbamate Adducts at Physiological Conditions PloS one 11:e0160491 doi:10.1371/journal.pone.0160491

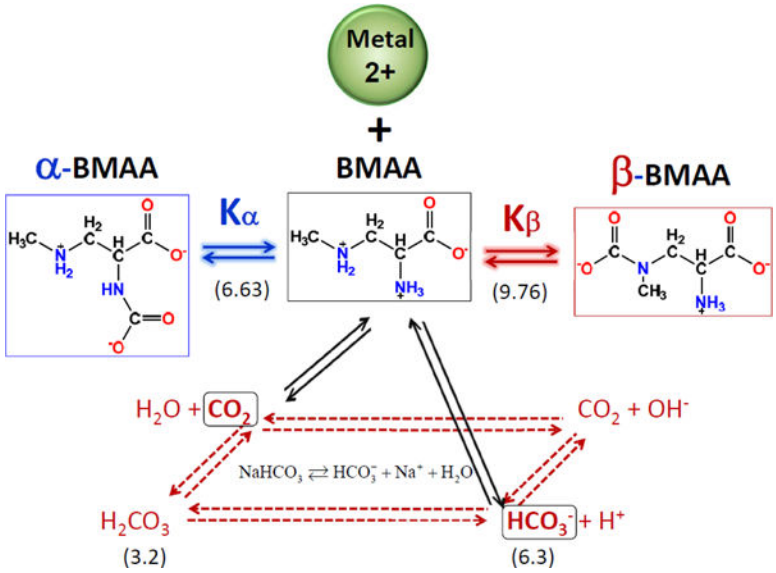

Figure 1:

Overview of the chemical equilibrium processes for the formation of the carbamates of BMAA and their interaction with the divalent metal ion. In the presence of sodium bicarbonate, at pH ~7.4, the formation of HCO_3^- and aqueous CO_2 that is essential for the carbamate is pre-formed by the various equilibria (red dashed arrows.) The reaction equilibria of HCO_3^- and aqueous CO_2 with BMAA (black arrows) and the equilibria leading to the formation of α-BMAA (blue arrows) and β–BMAA (red arrows), with the equilibrium constants of K_α and K_β, respectively, are shown schematically. The divalent metal ions (Mg^{2+}, Zn^{2+} or Cu^{2+}) further react with the BMAA or its carbamates to form their respective complexes. In this schematic representation, HCO_3^- and aqueous CO_2 are formed (pKa value of each reaction is given in parenthesis), and the formation of the carbamates is much slower than their complex formation with the divalent metal ions.

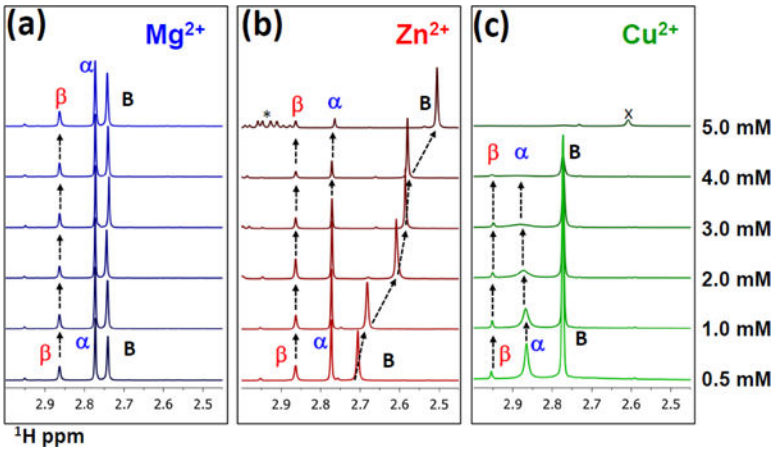

Figure 2:

Proton NMR spectral changes due to the interaction between BMAA and divalent metal ions. Methyl regions of the NMR spectra of 10 mM of BMAA and 200 mM of HCO_3^- (1:20) as a function of increasing concentration of (a) Mg^{2+}, (b) Zn^{2+} and (c) Cu^{2+} (noted at the right). The * represents chemically shifted resonances of BMAA, and 'x' represents additional low-intensity peaks appear at high metal ion concentrations.

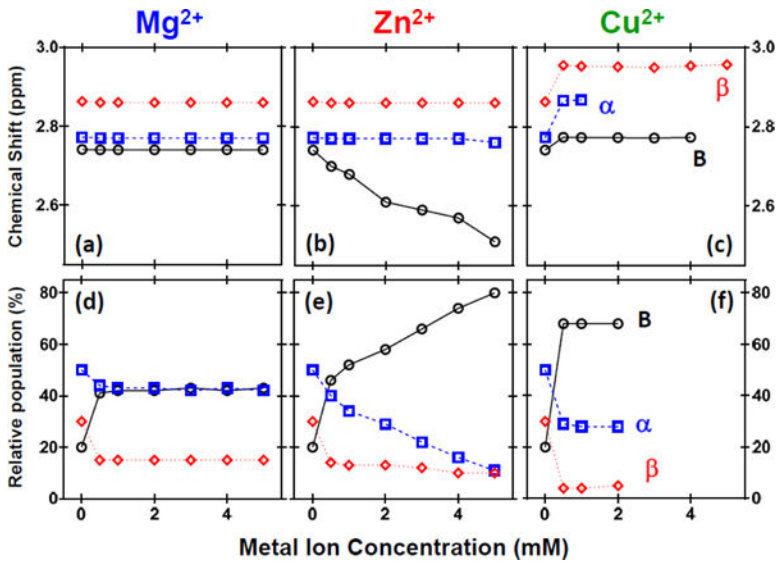

Figure 3:

Changes in the chemical shifts and populations of BMAA and its adducts with increasing metal ion concentrations. The top row shows the change in the chemical shifts of the methyl protons of BMAA (B) α-BMAA (α) and β-BMAA (β) as a function of increasing concentrations of Mg^{2+} (left column), Zn^{2+} (middle column) and Cu^{2+} (right column). The bottom shows the change in the relative population calculated by the integration of the peak areas. All the samples contain a 1:20 ratio of BMAA: HCO_3^-. The measured chemical shifts and estimated populations have a coefficient of variations <0.1 ppm and < 5%, respectively.

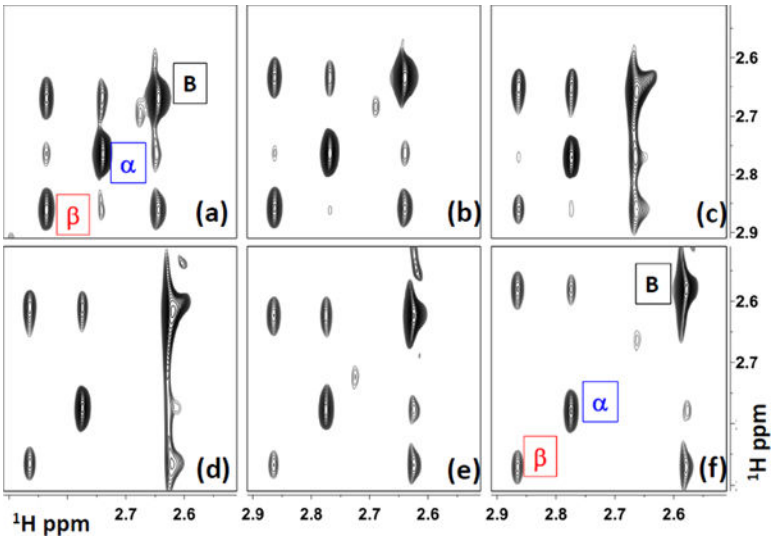

Figure 4:

Conformational exchange of BMAA and its carbamates with increasing concentration of Zn^{2+}. EXSY spectra of 10 mM BMAA (1:20 ratio with HCO_3^-) with increasing concentration Zn^{2+}; (a) 0.5 mM, (b) 1.0 mM, (c) 2.0 mM, (d) 3.0 mM, (e) 4.0 mM and (f) 5.0 mM. The diagonal peaks for the BMAA (B), α-BMAA (α) and β-BMAA (β) are identified in panels (a) and (f). Experiments were performed at 30 °C, pH 7.4 and a mixing time of 400 ms.

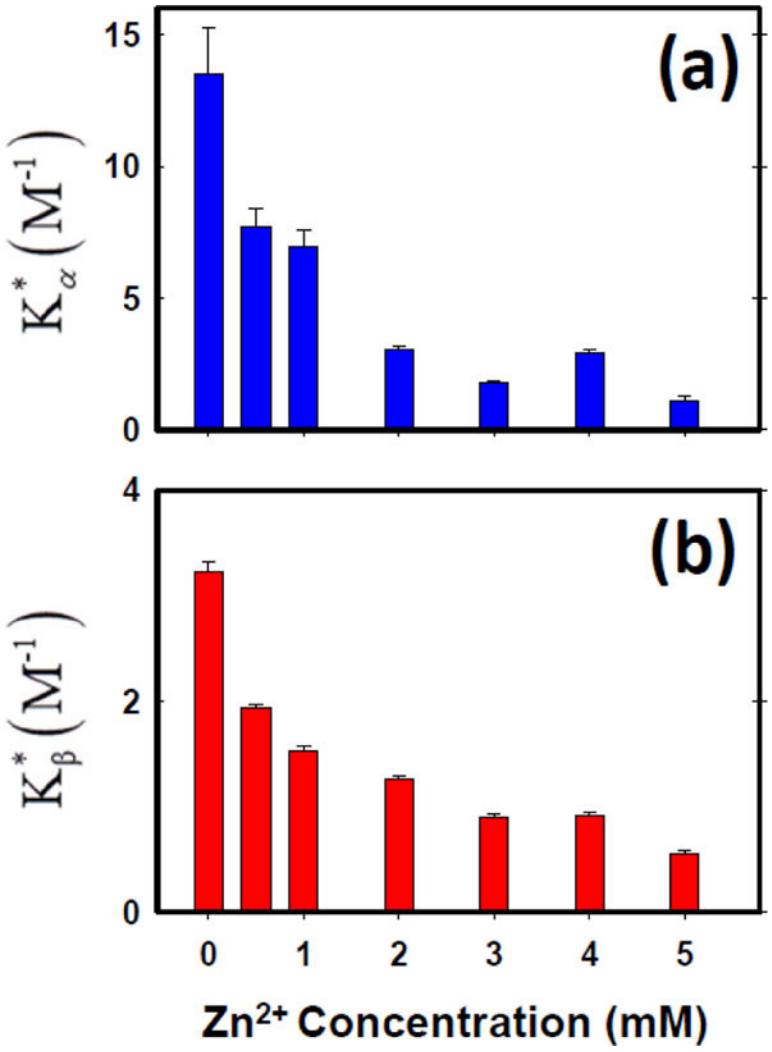

Figure 5:

Effect of Zn^{2+} concentration on the equilibria of BMMA and its carbamates. Plots of the Zn^{2+} concentration vs. the experimentally determined equilibrium constant of (a) α-BMAA carbamate and (b) β-BMAA carbamate formation.

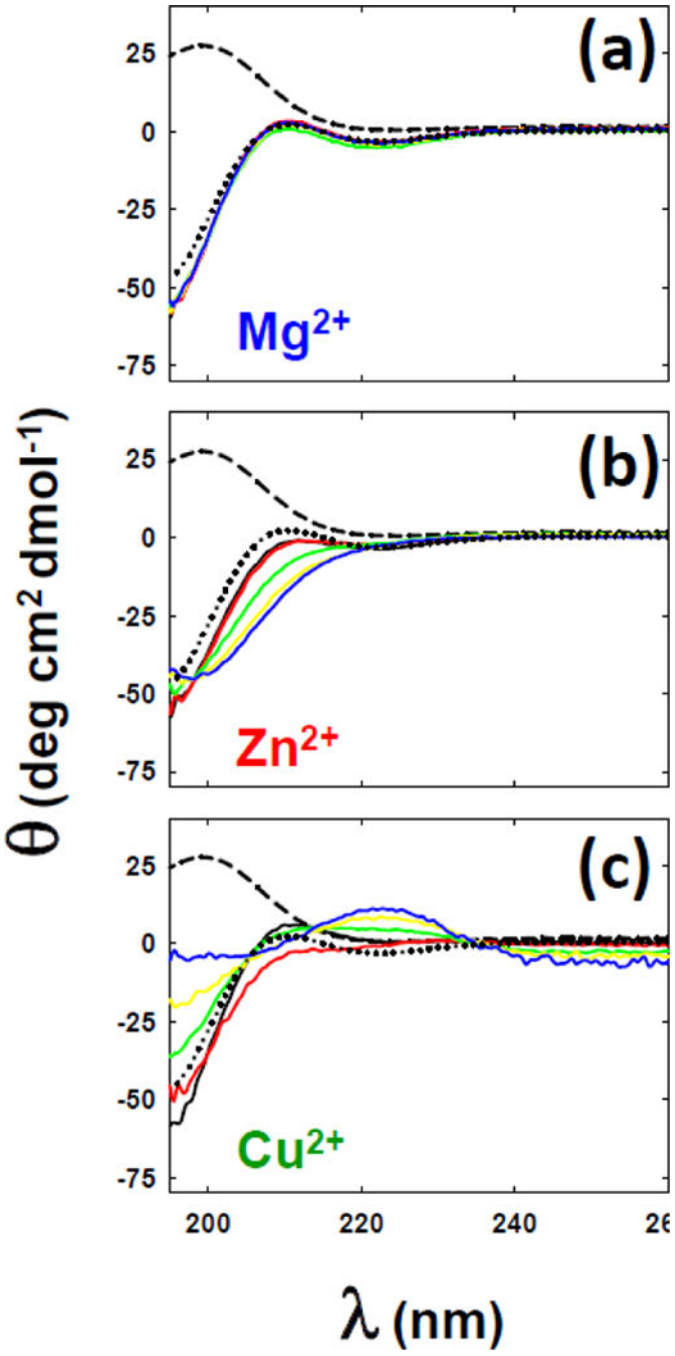

Figure 6:

Circular dichroism (CD) spectra of BMAA: HCO_3^- with varying concentrations of divalent metal ions. CD spectra of BMAA (dashed line, 10 mM), BMAA and HCO_3^- (dotted line, 1:20) as a function of increasing (a) Mg^{2+}, (b) Zn^{2+} and (c) Cu^{2+} ions. The concentration of the metal ions corresponds to black (0.5 mM), red (1.0 mM), green (2.0 mM), yellow (3.0 mM) and blue (4.0 mM).